

Electric Field Effect on the Vibration of Single CO Molecules in a Scanning Tunneling Microscope Junction

Shihai Yan and Jin Yong Lee*

Department of Chemistry, Institute of Basic Science, Sungkyunkwan University, Suwon 440-746, Korea

Jae Ryang Hahn*

Department of Chemistry and Research Institute of Physics and Chemistry, Chonbuk National University, Jeonju 561-756, Korea

Received: December 10, 2007; In Final Form: January 24, 2008

A low-temperature scanning tunneling microscope (STM) and *ab initio* calculations were used to study the electric field effect on the vibration of single CO molecules in an STM junction at 13 K. The vibrational energy of CO molecules adsorbed on silver atoms, measured by STM-based inelastic electron tunneling spectroscopy, depends on the direction of the electric field applied between the STM tip and the silver species. This characteristic can be explained by the charge separation model. The electric field modifies the binding characteristics of CO on silver as a result of a change in the charged states of the species, which leads to an increase (or a decrease) of the energies of the hindered rotation and the CO stretch on silver.

Inelastic tunneling spectroscopy performed using a scanning tunneling microscope (STM-IETS) has attracted great attention as a tool for chemical identification on the atomic scale.^{1–5} The vibrational spectrum of a single molecule adsorbed on a metal surface obtained by STM-IETS can provide insight into both the nature of the bonding and the local chemical environment. A great advantage of STM-IETS measurements is that the remarkable spatial resolution of the STM images permits changes in the molecular spectra to be correlated with variations in the local environment. Although vibrational features have been clearly revealed using STM, their behavior is much more complicated than that observed in conventional IETS experiments. Thus, it is very important to fully understand the details of STM-IETS and obtain more tunneling-active modes for different combinations of molecules and surfaces.

The vibrational energies obtained by STM-IETS may differ from those measured using conventional spectroscopic tools such as high-resolution electron energy loss spectroscopy (HREELS), infrared absorption and Raman techniques, inelastic neutron scattering, conventional IETS, and helium atom scattering spectroscopy; for example, the O–O stretching energy of O₂ molecules chemisorbed on a Ag(110) surface was found to be 82 meV using STM-IETS,⁵ whereas a value of 79 meV was obtained from HREELS measurements.⁶ One of the reasons for these differences is that all of the aforementioned techniques rely on a macroscopic number of molecules (i.e., ensemble average) to achieve detectable signal levels. The signal includes all the molecules, whose geometries and local environments can vary as a result of defects, steps, and the presence of coadsorbates. Another reason is that in the STM-IETS experiments, the adsorbates are normally subjected to a high electric field applied between the STM tip and the surface. If the nature of the adsorbates is modified by this electric field, their vibrational energy may change. Thus, we have studied the electric field

effect on the vibration of single CO molecules adsorbed on silver atoms (at 13 K) by using a low-temperature STM combined with *ab initio* calculations. We found that the vibrational energy of the CO molecules in the STM junction depended on the direction of the field applied between the STM tip and the sample, due to a modification of the binding characteristics of the CO species on the silver atoms.

STM imaging, manipulation, and vibrational spectroscopy measurements on single CO molecules adsorbed on Ag atoms were performed using a home-built variable-temperature STM housed in an ultrahigh-vacuum chamber with a base pressure of 2×10^{-11} Torr.^{7,8} The Ag(110) sample was prepared by 500 eV neon ion sputtering followed by annealing at 693 K. Polycrystalline tungsten tips were fabricated *in situ* by self-sputtering and annealing. The CO adsorbates were introduced into the chamber via a microcapillary array doser attached to a variable-leak valve at a sample temperature of 13 K. The CO coverage was kept below 0.01 monolayers (ML) to permit the investigation of individual, well-isolated molecules. Atomically resolved imaging of the silver atoms was achieved by transferring a CO molecule to the tip.^{9–11} All the experiments described here were performed at 13 K.

A single CO molecule adsorbed on a Ag(110) surface appears as an inverted sombrero (i.e., as a round depression with a protruding rim, see Figure 1a) in the topographical image obtained using a bare metallic tip. Atomically resolved images taken with a CO tip show that the CO species are bonded on atop sites. Controlled vertical transfer of the CO molecules between the tip apex and the surface was possible by applying an appropriate tunneling current and a suitable sample bias. The bare metallic tip was positioned over the CO molecules, thereby applying a tunneling current of 0.1 nA and a sample bias voltage of +70 mV. While keeping the feedback loop on, the bias was increased to +250 mV. The tunneling current was then ramped from 0.1 to 10 nA to induce transfer of the CO molecules to

* Corresponding authors. E-mail: jinyilee@skku.edu (J.Y.L.), jrhanh@chonbuk.ac.kr (J.R.H.).

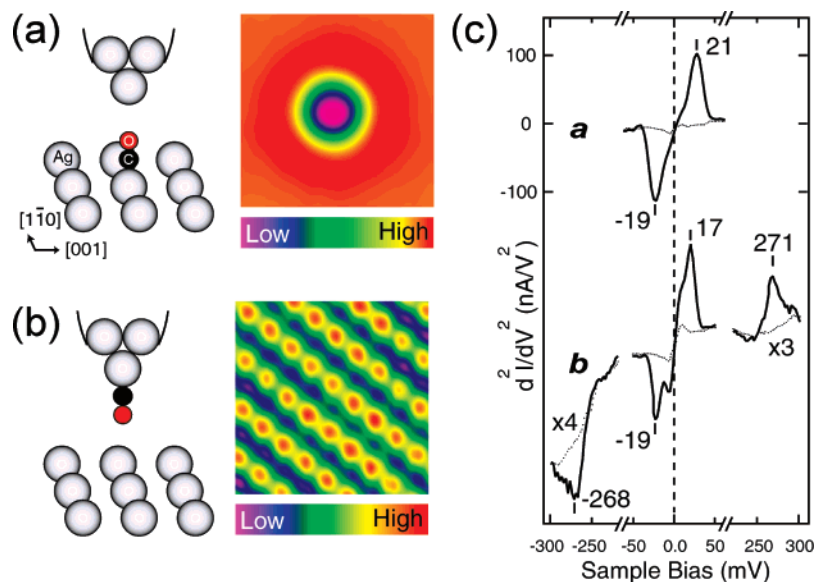


Figure 1. Topographical STM images of (a) a single CO molecule adsorbed on a Ag(110) surface (obtained by using a bare metallic tip) and (b) the Ag(110) surface (obtained by using a CO-terminated tip at 13 K). Schematic diagrams are also shown on the left-hand side. The scan area is $20 \times 20 \text{ \AA}^2$. Both images were obtained at a sample bias of 70 mV and a tunneling current of 1 nA. (c) STM-IETS spectra of CO adsorbed on the surface (curve a) and on the STM tip (curve b). The dotted lines are background spectra taken on a clean silver surface using a bare metallic STM tip. A dwell time of 300 ms (per 2.5 mV step) and an rms bias modulation of 7 mV at 200 Hz were used for recording the spectra. Tunneling gaps were set with a 70 mV sample bias and a 1 nA tunneling current. The line markers indicate the positions of the vibrational modes. The positions of the peak and the dip were determined by fitting the spectra to Gaussian functions (with an uncertainty of 1 meV).

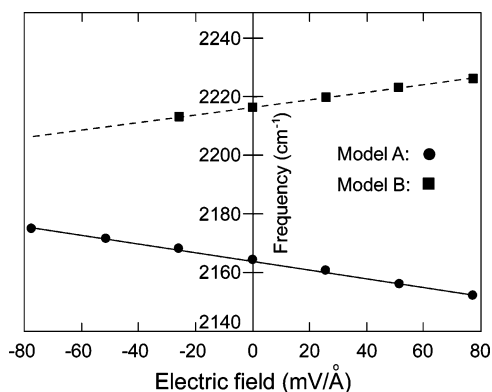


Figure 2. Vibrational energy of the C–O stretch as a function of the applied electric field. Model A: CO adsorbed on the Ag(110) surface. Model B: CO adsorbed on the STM tip.

the tip. The thus obtained CO tip was able to consistently resolve surface silver atoms (see Figure 1b).

The vibrational spectra shown in Figure 1c were obtained in STM-IETS experiments performed on CO species adsorbed on the surface (curve a) and on the STM tip (curve b). The background structure varied depending on the state of the tip. Thus, we showed the background spectra (dotted lines), which were taken on a clean surface using a bare metallic tip in Figure 1. A high resolution—with 0.5 mV steps and a root-mean-square (rms) modulation of 5 mV—was used in the spectra to determine the isotope shifts with an accuracy of 0.3 mV. The spectrum of the CO species adsorbed on the Ag(110) surface (curve a) reveals a peak (dip) at positive (negative) bias voltages, which can be assigned to the hindered rotational mode. The voltage position of the peak is higher in magnitude (by 2 mV) than that of the dip. The CO molecules adsorbed on the silver surface at 13 K are moved laterally when the sample bias is increased toward the C–O stretching energy, thus precluding the measurement.

Curve b in Figure 1c exhibits two peaks (dips) at positive (negative) sample bias voltages, the hindered rotational mode

being observed at -19 and $+17$ mV. In contrast to curve a, the voltage position of the dip is higher in magnitude (by 2 mV) than that of the peak. An additional vibrational mode is observed at sample bias voltages of -268 and $+271$ mV. This mode can be assigned to the C–O stretching vibration. It should be mentioned that the bare metallic tip can be terminated with Ag atoms prior to transferring a CO molecule to the STM tip. Physical contacts made with the silver surface during the in situ tip-sharpening process can lead to the attachment of Ag atoms to the tip. The hindered translation of the CO species (several millielectronvolts) and the symmetric CO–Ag stretching modes were not resolved by STM-IETS.

It is interesting that the vibrational energies of CO at positive and negative sample bias voltages are asymmetric. In the case of the hindered rotational mode, the voltage position of the peak (dip) is higher in magnitude, by 2 mV, than that of the dip (peak) for a CO molecule adsorbed on the surface (STM tip). In the case of the C–O stretching mode, the voltage position of the peak is higher in magnitude, by 3 mV, than that of the dip. This asymmetry in the voltage position was not observed in the case of the C–H,^{1,2,12,13} O–O,⁵ the asymmetric Ag–O₂ stretching vibrations,^{5,9} or the (external or frustrated) benzene–Ag(110) vibrations^{14,15}—all recorded using STM-IETS—but was observed in the case of CO molecules adsorbed on Ag and Cu surfaces.^{9–11,16} A CO molecule adsorbed on a surface has a high dipole moment along its molecular axis. Thus, the asymmetry in the vibrational energy can be attributed to either a change in the interaction of the CO molecule on the silver surface at different field directions or an electrostatic effect (Stark shift).

To understand the changes in the CO stretching energy in the presence of an external electric field, we carried out ab initio calculations for model systems composed of CO molecules adsorbed on a Ag(110) surface and on the STM tip (coated with Ag atoms). According to the CO adsorption sites revealed in the STM images, two model systems were considered in the calculations: model A, the CO species is adsorbed on the Ag(110) surface (see Figure 1a), and model B, the CO species is

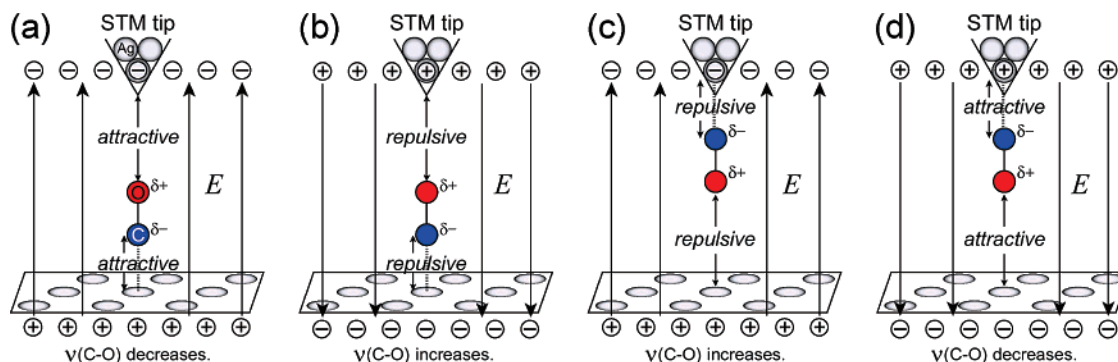


Figure 3. Charge separation diagrams of the HOMO structure of CO under positive and negative sample bias voltages in models A and B: (a) sample positive/model A, (b) sample negative/model A, (c) sample positive/model B, (d) sample negative/model B. In (a) and (d), due to the attractive electrostatic interactions between $C^{\delta-}$ and the positive charges on the silver surface and between $O^{\delta+}$ and negative charges on the silver-coated STM tip, the C–O bond is weakened, and thus the stretching frequency decreases as the field strength increases. Oppositely, in (b) and (c), the stretching frequency increases as the field strength increases. The gray, red, and blue spheres represent silver, oxygen, and carbon atoms, respectively.

adsorbed on the silver tip (see Figure 1b). In both models, CO is bonded on atop sites. A tetrahedral geometry was used to mimic the STM tip, and 14 Ag atoms were used to mimic the Ag(110) surface. The presently adapted cluster model for the metal surface in the external electric field may not exactly describe the experimentally created electric field between the STM tip and the extended silver surface. However, our main objective of the present study is to understand the CO frequency changes observed in the experiment at the first stage of theoretical aspect because there is no previous trial. In addition, the cluster models have often successfully been used to study the stability and electronic properties of adsorbed molecules on silicon or metal surfaces.^{17–22} In this regard, our cluster model in the external electric field may give some physical insight for the experimentally observed phenomenon.

For the fixed Ag configurations, the CO bond length was optimized with density functional theory employing the Becke's three-parameter Lee–Yang–Parr (B3LYP) exchange correlation functions using the 6-311+G* basis sets for CO molecule and the LanL2DZ basis sets for Ag atoms.²³ The C–O stretching vibrations were calculated after performing the geometry optimizations. All calculations were carried out using a suite of Gaussian 03 programs.²⁴ The Gaussian programs have been successful to explain the vibrational frequencies of molecules in bare gas or complex systems in comparison with experiments.^{25,26}

The distance between the surface and the tip was assumed to be 5 to ~ 10 Å, although the exact separation cannot be defined in the experiments. The electric field strength was estimated to be 7 to ~ 14 mV/Å. In our calculations, we used electric field strengths between -77 and $+77$ mV/Å to study the dependence of the CO stretching energy on the field. Here, a positive (negative) electric field means that the direction of the applied electric field is from the silver surface (STM tip) to the STM tip (silver surface). It should be noted that the field dependence of the CO stretching energy is remarkably influenced by the geometry of the tip. When the tip geometry was slightly modified—by elongating the bottom Ag atom downward—a field dependence of the CO stretching energy was observed.

In the case of model A, the CO stretching energies were calculated to be 2175.2, 2171.7, 2167.9, 2164.1, 2160.3, 2156.2, and 2152.2 cm^{-1} for field strengths of -77.16 , -51.44 , -25.72 , 0.0 , 25.72 , 51.44 , and 77.16 mV/Å, respectively (see Figure 2), that is, the stretching energies were observed to decrease with increasing field strength. In the case of model B, the opposite trend was observed (i.e., the stretching energy increased

with increasing field strength). This result is consistent with the experimental observations (curve b in Figure 1c), the vibrational frequencies being 268 meV at negative bias voltages and 271 meV at positive ones. Curve b was obtained from a molecular system similar to model B. In other words, the CO stretching energy was observed to be higher (by 3 meV or ≈ 24 cm^{-1}) at positive voltages than at negative ones for the CO species adsorbed on the STM tip. Our calculated results are consistent with the experimentally observed field dependence, although quantitative concordance is still lacking. We believe that such a quantitative comparison may not be possible yet, because neither the tip geometry nor the field strength between the surface and the tip can be accurately defined. In general, the CO vibrational frequencies in model B are higher than those in model A, which can be attributed to the fact that the CO molecules adsorb more strongly on the silver surface than on the STM tip.

Recently, the orbital energy changes under the applied electric field for benzene molecule were studied.²⁷ The highest occupied molecule orbital (HOMO) presumably plays the most significant contributions to the charge separations (or polarization changes) under the applied field because unoccupied MOs have little effect on the charge density. Thus, the field dependence of the CO vibration energy can be explained using the charge separation model in the HOMO structures of the CO molecules in the STM junction. In addition, from the MO theory, it is well-established that the HOMO electrons of the CO molecule mainly come from the carbon lone pair orbital though the oxygen is more electronegative than the carbon.²⁸ Thus, the electrostatic environments around the CO molecules and the charge separation of the HOMO of the CO molecule can be described as shown in Figure 3 when the external electric field (E) is applied to models A and B. In the case of a positive voltage (applied to the surface) in model A (see Figure 3a), the attractive electrostatic interactions between the negatively charged carbon atom and the positively charged silver surface weaken the CO bond, thus reducing the CO stretching energy. In the case of a negative surface voltage (Figure 3b), the same rationale gives rise to an increase of the CO stretching energy. For model B, the calculated field dependence of the CO stretching energy can be explained in the same way. The field dependence of the hindered rotational energy can also be explained by the same charge separation model. Weakening of the carbon–silver bond causes a decrease in the hindered rotational energy. Thus, a lower rotational energy is observed

in the STM-IETS spectra for model A under a negative sample bias and for model B under a positive one (see Figure 1c).

The asymmetry in the energy of the CO vibrations on silver at positive and negative bias voltages may also be due to an electrostatic effect (Stark shift). For the C–O stretch on a Cu(001) surface,²⁹ it was found that $dv/dE \approx 10 \text{ meV/V} \cdot \text{\AA}^{-1}$. Assuming planar electrodes and a tunneling gap of 5 Å, the energy difference between the C–O stretching peaks of the negative and the positive bias should be approximately 1 meV. For the hindered rotational mode of CO on Cu(001) and Cu(110),¹⁶ 3 meV shift was due to the Stark effect, the approximations above suggest that $dv/dE \approx 200 \text{ meV/V} \cdot \text{\AA}^{-1}$, which is an order of magnitude greater than the theoretical estimates.³⁰ It should be noted that when the Ag(110) surface and the tip are absent in our calculations, the change in the CO stretching energy is negligible in the field range between -1.0 and $+1.0 \text{ V/\AA}$. In addition, if the applied field is very strong (regardless of its direction), the bond length of the bare CO molecule increases, and the vibrational energy decreases gradually. This behavior is different from that observed for a CO molecule adsorbed on the silver surface or on the STM tip. Therefore, we suggest that the STM junction has a significant influence on the change of the molecular vibration under the applied electric field. The asymmetry of the vibration energy at positive and negative bias voltages is likely a result of the electrostatic interactions between the CO molecule and the surface/STM tip.

In summary, we measured the vibrational energies of single CO molecules inside an STM junction by means of STM-IETS at 13 K. The vibrational energies of the CO stretch and the hindered rotation of the Ag–CO bond were both found to change with varying bias polarity. Our calculations reveal that the vibrational energy of the CO species in the STM-IETS experiments is affected by the field applied between the surface and the tip. The electric field modifies the binding characteristics of the CO molecule on the silver atom, which leads to an increase or decrease in the energies of both the hindered rotation of the CO on Ag and the C–O stretching. The change in the binding characteristics caused by the presence of the STM junction seems to be a more influential factor for this energy variation than the electrostatic Stark effect.

Acknowledgment. This work was supported by the Korea Science and Engineering Foundation (KOSEF), the Ministry of Science and Technology (MOST, Grant No. R11-2007-012-02001-0), and the Korea Research Foundation Grant (MOE-HRD, Basic Research Promotion Fund, Grant No. KRF-2006-311-C00082).

References and Notes

- (1) Stipe, B. C.; Rezaei, M. A.; Ho, W. *Science* **1998**, *280*, 1732.
- (2) Ho, W. *J. Chem. Phys.* **2002**, *117*, 11033.
- (3) Komeda, T. *Prog. Surf. Sci.* **2005**, *78*, 41.
- (4) Ueba, H. *Surf. Rev. Lett.* **2003**, *10*, 771.
- (5) Hahn, J. R.; Lee, H. J.; Ho, W. *Phys. Rev. Lett.* **2000**, *85*, 1914.
- (6) Sexton, B. A.; Madix, R. J. *Chem. Phys. Lett.* **1980**, *76*, 294.
- (7) Hahn, J. R. *Bull. Korean Chem. Soc.* **2005**, *26*, 1071.
- (8) Hahn, J. R.; Jeong, H.; Jeong, S. *J. Chem. Phys.* **2005**, *123*, 244702.
- (9) Hahn, J. R.; Ho, W. *Phys. Rev. Lett.* **2001**, *87*, 196102.
- (10) Hahn, J. R.; Ho, W. *Phys. Rev. Lett.* **2001**, *87*, 166102.
- (11) Lee, H. J.; Ho, W. *Science* **1999**, *286*, 1719.
- (12) Kim, Y.; Komeda, T.; Kawai, M. *Phys. Rev. Lett.* **2002**, *89*, 126104.
- (13) Hahn, J. R.; Ho, W. *J. Chem. Phys.* **2006**, *124*, 204708.
- (14) Pascual, J. I.; Jackiw, J. J.; Kelly, K. E.; Conrad, H.; Rust, H.-P.; Weiss, P. S. *Phys. Rev. Lett.* **2001**, *86*, 1050.
- (15) Pascual, J. I.; Jackiw, J. J.; Song, Z.; Weiss, P. S.; Conrad, H.; Rust, H.-P. *Surf. Sci.* **2002**, *502–503*, 1.
- (16) Lauhon, L. J.; Ho, W. *Phys. Rev. B* **1999**, *60*, R8525.
- (17) Schneider, W. F.; Hass, K. C.; Ramprasad, R.; Adams, J. B. *J. Phys. Chem.* **1996**, *100*, 6032.
- (18) Loh, Z.-H.; Kang, H. C. *J. Chem. Phys.* **2000**, *112*, 2444.
- (19) Hu, Q.-M.; Reuter, K.; Scheffler, M. *Phys. Rev. Lett.* **2007**, *98*, 176103.
- (20) Zhou, J.; Li, Z.-H.; Wang, W.-N.; Fan, K.-N. *J. Phys. Chem. A* **2006**, *110*, 7167.
- (21) Festa, G.; Cossi, M.; Barone, V.; Cantele, G.; Ninno, D.; Iadonisi, G. *J. Chem. Phys.* **2005**, *122*, 184714.
- (22) Li, B.; Michaelides, A.; Scheffler, M. *Phys. Rev. Lett.* **2006**, *97*, 046802.
- (23) Becke, A. D. *J. Chem. Phys.* **1993**, *98*, 5648.
- (24) Frisch, M. J.; Trucks, G. W.; Schlegel, H. B.; Scuseria, G. E.; Robb, M. A.; Cheeseman, J. R.; Montgomery, J. A., Jr.; Vreven, T.; Kudin, K. N.; Burant, J. C.; Millam, J. M.; Iyengar, S. S.; Tomasi, J.; Barone, V.; Mennucci, B.; Cossi, M.; Scalmani, G.; Rega, N.; Petersson, G. A.; Nakatsuji, H.; Hada, M.; Ehara, M.; Toyota, K.; Fukuda, R.; Hasegawa, J.; Ishida, M.; Nakajima, T.; Honda, Y.; Kitao, O.; Nakai, H.; Klene, M.; Li, X.; Knox, J. E.; Hratchian, H. P.; Cross, J. B.; Bakken, V.; Adamo, C.; Jaramillo, J.; Gomperts, R.; Stratmann, R. E.; Yazyev, O.; Austin, A. J.; Cammi, R.; Pomelli, C.; Ochterski, J. W.; Ayala, P. Y.; Morokuma, K.; Voth, G. A.; Salvador, P.; Dannenberg, J. J.; Zakrzewski, V. G.; Dapprich, S.; Daniels, A. D.; Strain, M. C.; Farkas, O.; Malick, D. K.; Rabuck, A. D.; Raghavachari, K.; Foresman, J. B.; Ortiz, J. V.; Cui, Q.; Baboul, A. G.; Clifford, S.; Cioslowski, J.; Stefanov, B. B.; Liu, G.; Liashenko, A.; Piskorz, P.; Komaromi, I.; Martin, R. L.; Fox, D. J.; Keith, T.; Al-Laham, M. A.; Peng, C. Y.; Nanayakkara, A.; Challacombe, M.; Gill, P. M. W.; Johnson, B.; Chen, W.; Wong, M. W.; Gonzalez, C.; Pople, J. A. *Gaussian 03*, revision A1; Gaussian Inc.: Pittsburgh, PA, 2003.
- (25) (a) Lee, J. Y.; Hahn, O.; Lee, S. J.; Choi, H. S.; Shim, H.; Mhin, B. J.; Kim, K. S. *J. Phys. Chem.* **1995**, *99*, 1913. (b) Lee, J. Y.; Hahn, O.; Lee, S. J.; Mhin, B. J.; Lee, M. S.; Kim, K. S. *J. Phys. Chem.* **1995**, *99*, 2262. (c) Lee, J. Y.; Lee, S. J.; Kim, K. S. *J. Chem. Phys.* **1997**, *107*, 4112.
- (26) (a) Tarakeshwar, P.; Lee, S. J.; Lee, J. Y.; Kim, K. S. *J. Chem. Phys.* **1998**, *108*, 7217. (b) Lee, J. Y.; Kim, J.; Lee, H. M.; Tarakeshwar, P.; Kim, K. S. *J. Chem. Phys.* **2000**, *113*, 6160. (c) Rhee, S. K.; Kim, S. H.; Lee, S.; Lee, J. Y. *J. Chem. Phys.* **2004**, *297*, 21. (d) Song, J. H.; Kim, J.; Seo, G.; Lee, J. Y. *J. Mol. Struct. (THEOCHEM)* **2004**, *686*, 147.
- (27) Choi, Y. C.; Kim, W. Y.; Park, K.-S.; Tarakeshwar, P.; Kim, K. S.; Kim, T.-S.; Lee, J. Y. *J. Chem. Phys.* **2005**, *122*, 094760.
- (28) Purcell, K. F.; Kotz, J. C. *An Introduction to Inorganic Chemistry*; Saunders Golden Sunburst Series, 119; Saunders College Publishing, Holt, Rinehart and Winston: 1980.
- (29) Bagus, P. S.; Nelin, C. J.; Müller, W.; Philpott, M. R.; Seki, H. *Phys. Rev. Lett.* **1987**, *58*, 559.
- (30) Head-Gordon, M.; Tully, J. C. *J. Chem. Phys.* **1993**, *175*, 37.